The Journal of Physical Chemistry A

 VOLUME 103, NUMBER 19, MAY 13, 1999

ARTICLES

Excited-State Kinetics of the Hydrophobic Probe Nile Red in Membranes and Micelles

M. M. G. Krishna*

Department of Chemical Sciences, Tata Institute of Fundamental Research, Homi Bhabha Road, Colaba, Mumbai 400005 India

Received: December 4, 1998

Nile red is a widely used hydrophobic dye for probing the structure, dynamics, and environment in many biological and microheterogeneous systems. This paper reports emission-wavelength-dependent fluorescence intensity decay of Nile red in membranes and micelles. Global analysis of these multiple fluorescence decays reveals a double-exponential decay with negative amplitudes for the short-lifetime component at longer emission wavelengths. This indicates an excited-state kinetics leading to the formation of a new species in the excited state from the initially excited state. In both the cases, the short lifetime corresponds to that of the initially excited species. This excited-state kinetics is also observed in the case of viscous organic solvents such as 1-octanol and glycerol and is attributed to that of an excited-state solvent relaxation.

Introduction

Nile red (Nile blue A oxazone) is a commonly employed hydrophobic dye in the study of biological systems such as membranes,[1] micelles,[2] reverse micelles[3] and proteins,[4] and for staining biological tissues.[5] This dye has also been widely used in the studies of various organized assemblies such as zeolites,[6] liquid crystals,[7] LB films,[8] and planar supported membranes.[9] The fluorescence properties of Nile red highly depend on the polarity of the probe environment.[10] A twisted intramolecular charge transfer (TICT) state has been proposed to account for the polarity-sensitive fluorescence of Nile red.[6,11] However, unlike most other TICT molecules, dual fluorescence was not observed, and hence, the TICT of Nile red was proposed to be nonemissive.[6] In all the above reports, a single emissive state was assumed to explain the fluorescence properties of Nile red. Interestingly, wavelength-dependent fluorescence decay with negative amplitudes for a short-lifetime component indicating excited-state kinetics has not been reported in the above studies.

This paper reports the observation of wavelength-dependent fluorescence intensity decay of Nile red in egg PC vesicles, SDS micelles, and viscous alcohols, and this is attributed to that of the excited-state solvent relaxation of Nile red.

Materials and Methods

Nile red, whose molecular structure is shown in Figure 1, was obtained from Exciton Inc.. The purity was checked using thin-layer chromatography on silica plates in different solvent mixtures as described in ref 12. The solvents used as eluents include chloroform, acetonitrile/water (99:1), acetonitrile/tetrahydrofuran (80:20) and chloroform/methanol (95:5). Single spots were observed on silica plates, indicating that Nile red is pure. Fluorescence measurements were carried out on Nile red incorporated in egg PC (L-α-phosphatidylcholine from fresh egg yolk, Sigma Chemical Co.) vesicles and SDS (sodium dodecyl sulfate, Sigma Chemical Co.) micelles in 10 mM NaH_2PO_4, pH 7.4 buffer. The sonicated egg PC liposomes were prepared as described in ref 13. The lipid concentration used in these experiments was 0.3 mg/mL (~0.42 mM). SDS micelles were prepared by stirring the surfactant in warm deionized water for 1 h. The dye (0.77 μM) was added from the stock solution made in ethanol to the samples and kept overnight. The final samples

* To whom correspondence should be addressed. E-mail: mmg@tifr.res.in. Fax: 091-22-215 2110/2181. Phone: 091-22-215 2971/2979, ext 2526.

10.1021/jp984620m CCC: $18.00
Published on Web 04/22/1999

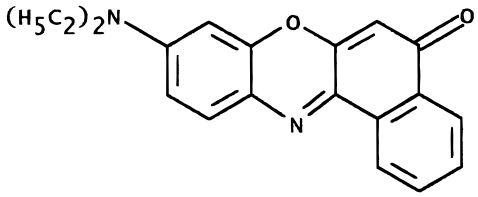

Figure 1. Chemical structure of Nile red.

contain less than 1% v/v ethanol. The dye-to-lipid ratio was kept approximately at 1:543, and the dye-to-micelle ratio was kept nearly at 1:1272. Nile red is nearly insoluble in water and becomes nonfluorescent within 20−25 min.[12] In the presence of membranes and micelles, Nile red partitions completely into the hydrophobic phase at the concentration ratios maintained here[13,2a] and the dye is very stable under these conditions. All measurements were carried out in air-saturated solutions at room temperature (25 °C). All solvents used in the fluorescence studies were of spectroscopic grade and tested to be free of any fluorescence impurities.

The steady-state fluorescence intensity measurements were carried out on a SPEX Fluorolog 1681 T format spectrofluorophotometer. The time-resolved fluorescence measurements were made using a high repetition rate (800 kHz) picosecond laser coupled with a time-correlated single-photon-counting (TCSPC) setup described elsewhere,[14] using a microchannel plate photomultiplier (Hamamatsu 2809). The samples were excited either at 570 or at 445 nm. The excitation wavelength of 570 nm was obtained from a cavity-dumped, mode-locked, picosecond rhodamine 6G dye laser (Spectra Physics) synchronously pumped by the frequency-doubled output (532 nm) of a CW, mode-locked Nd:YAG laser (Spectra Physics series 3000). The other excitation wavelength at 445 nm was a frequency-doubled output of a mode-locked picosecond Spectra Physics Ti:sapphire Tsunami laser pumped by a diode-pumped CW Spectra Physics Millenia X Nd:vanadate laser (532 nm). The sample was excited with vertically polarized light, and the fluorescence decay was collected with an emission polarizer kept at the magic angle (∼54.7°) with respect to the excitation polarizer for measuring lifetimes. The emission monochromator used was an *f*/4 monochromator (model 121S15MV, Edinburgh Instruments) with a band-pass of 1.4 nm for a slit width of 250 μm. The instrument response function (IRF) was recorded using a nondairy creamer scattering solution. The full width at half-maximum (fwhm) of IRF is about 200 ps. The fluorescence decays were collected over 512 data channels with either 75.68 or 37.84 ps as the time per channel. Typical peak count in the emission decay for fluorescence intensity measurements was about 10 000. Proper filters (RG 610 or GG 475 Schott color filter glasses) were used on the emission side to cut off any scattered excitation light (570 or 445 nm).

The experimentally measured fluorescence decay data is a convolution of the instrument response function (IRF) and the intensity decay function (single or multiexponential). The popular method of deconvolution of individual fluorescence decay data is by the method of iterative reconvolution using the IRF and an assumed decay function whose parameters are improved in successive iterations. The iterative procedure for the optimization of the parameters (lifetimes, amplitudes, and shift) by the Levenberg−Marquardt algorithm has been described earlier.[14]

The fluorescence decays of Nile red in egg PC vesicles and SDS micelles were analyzed by discrete exponential analysis. In discrete exponential analysis, the intensity decay function was fitted to a multiexponential function,

$$I(t) = \sum_i \alpha_i \exp(-t/\tau_i) \quad (1)$$

where α_i and τ_i are the amplitudes and the lifetimes. The goodness of the fits was judged by the χ^2 value (close to 1) and the random residual distribution.

The fluorescence intensity decays were collected as a function of the emission wavelength over the emission spectra of Nile red in egg PC vesicles and SDS micelles at an interval of 5 nm with the excitation wavelength at 570 nm. These decays were globally analyzed to obtain the lifetimes that are common to all the decays and the amplitudes varying with the wavelength. Global analysis for the simultaneous fitting of multiple fluorescence decays is a very useful technique for the accurate estimate of the parameters that are common to all the decay data sets.[15] The main advantage of this method is the reduction in the number of free parameters to be optimized and hence increases the confidence limits on the thus obtained parameters.

Results and Discussion

Nile red in methanol exhibits single-exponential fluorescence decay at all emission wavelengths from 580 to 750 nm with a lifetime of 2.88 ns. The single-exponential decay confirms the purity of the sample and the presence of a single emitting species in the excited state.

Nile Red in Egg PC Vesicles. The fluorescence decay of Nile red in egg PC vesicles is strongly emission-wavelength-dependent. The fluorescence emission maximum is at 630 nm. Figure 2 shows the fluorescence decays obtained at three emission wavelengths: 580, 630, and 750 nm. The fluorescence decay collected at the blue end of the emission spectrum (580 nm) shows a short-lifetime component in addition to the long-lifetime component, whereas the fluorescence decay collected at the red end of the emission spectrum (750 nm) shows a rising component. Hence, a single-exponential fluorescence decay cannot explain the fluorescence decay kinetics of Nile red in egg PC vesicles at all emission wavelengths. A double-exponential global analysis of multiple fluorescence decays collected as a function of emission wavelength from 580 to 750 nm gave two lifetimes of 1.26 and 3.88 ns with the amplitudes varying with the emission wavelength. The amplitudes of the short-lifetime component (1.26 ns) are positive at shorter emission wavelengths and become negative at longer emission wavelengths (λ_{em} > 630 nm) as shown in Figure 3A. The observation of negative amplitudes indicates excited-state kinetics leading to a new emitting state from the initially excited state.

Nile Red in SDS Micelles. The fluorescence of Nile red in SDS micelles is also wavelength-dependent as in the case of Nile red in egg PC vesicles. The emission maximum occurs at 640 nm for Nile red in SDS. The global analysis of multiple fluorescence decays collected at wavelengths from 585 to 750 nm fit to a double-exponential function with the lifetimes 0.68 and 2.53 ns. The amplitudes of the two lifetimes vary with the emission wavelength, and the amplitudes of the short-lifetime component (0.68 ns) become negative at emission wavelengths λ_{em} > 640 nm (Figure 3B). The observation of negative amplitudes indicates an excited-state kinetics in the case of Nile red in SDS micelles.

Fluorescence Decay Kinetics and Species-Associated Spectra. Observation of two lifetimes and the negative amplitudes for one of the lifetime components in the case of Nile red in egg PC vesicles and SDS micelles indicates excited-state kinetics during the lifetime of the initially excited state leading to a new

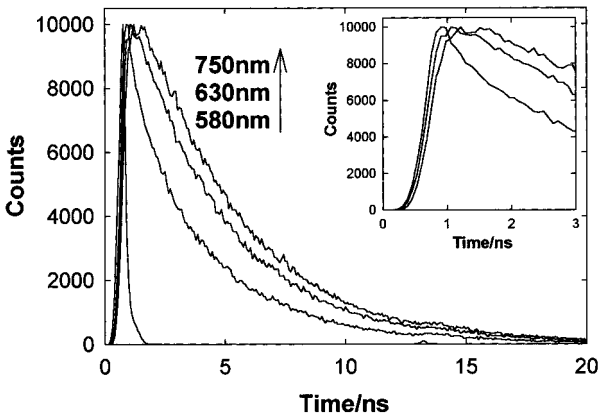

Figure 2. Fluorescence intensity decays of Nile red (0.77 μM) in egg PC (0.42 mM) at emission wavelengths 580, 630, and 750 nm with the excitation wavelength of 570 nm. The instrument response function (IRF) is also indicated in the figure. The inset shows the three fluorescence decays plotted over a more expanded time scale to indicate the differences in the rising edges.

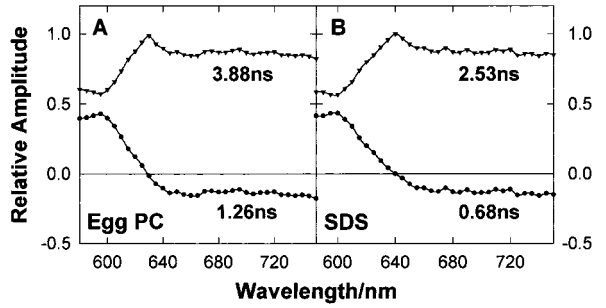

Figure 3. Relative amplitudes of the two lifetimes obtained by the global analysis of multiple fluorescence intensity decays collected at different emission wavelengths with the excitation wavelength of 570 nm in the case of Nile red (0.77 μM) in (A) egg PC (0.42 mM) vesicles and (B) SDS (69 mM) micelles.

emitting state. Analytical equations were derived for the fluorescence intensity decays and species-associated spectra (SAS) in the case of two-state kinetics in the excited state.

Figure 4 shows the model for the excited-state kinetics. Let A* be the initially excited species and B* be the newly formed species. In the case of irreversible reaction of A* (Figure 4A), let k_A and k_B represent the rate constants (radiative and nonradiative processes) at which the species A* and B* emit and k_{AB} be the rate of formation of B* from A*. In this kinetic scheme, the intensity decay equation can be obtained as

$$I_\lambda(t) = a_\lambda[\mathrm{A}^*]_t + b_\lambda[\mathrm{B}^*]_t$$

i.e.,

$$I_\lambda(t) = [\mathrm{A}^*]_0\left[\left(a_\lambda + \frac{b_\lambda k_{AB}\tau_A\tau_B}{\tau_A - \tau_B}\right)\exp\left(-\frac{t}{\tau_A}\right) - \frac{b_\lambda k_{AB}\tau_A\tau_B}{\tau_A - \tau_B}\exp\left(-\frac{t}{\tau_B}\right)\right] \quad (2)$$

where a_λ and b_λ are wavelength-dependent spectral amplitudes of A* and B* and $\tau_A = (k_A + k_{AB})^{-1}$ and $\tau_B = k_B^{-1}$. When the lifetime of the initially excited species τ_A is longer than that of the newly formed species τ_B, eq 2 predicts negative amplitudes for the short-lifetime component τ_B at all emission wavelengths. In the other case where $\tau_B > \tau_A$, the negative amplitudes for the short-lifetime component τ_A occur at longer emission wavelengths where $a_\lambda < b_\lambda k_{AB}\tau_A\tau_B/(\tau_B - \tau_A)$, i.e., at the

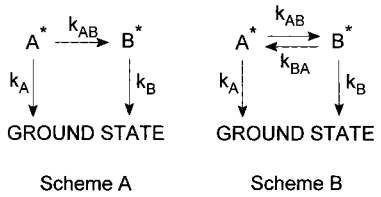

Figure 4. Model for the excited-state kinetics of Nile red: (A) irreversible reaction in the excited state; (B) reversible reaction in the excited state. A* and B* represent the initially excited and newly formed species in the excited state.

wavelengths where the emission from the newly formed species dominates over the emission from the initially excited species.

In the case of Nile red in egg PC vesicles and SDS micelles, negative amplitudes for the short-lifetime component occurs only at the long emission wavelengths. Hence, in both these cases, the short lifetime can be associated with that of the initially excited species and the long lifetime with that of the newly formed species.

If α_A and α_B represent the amplitudes of the two exponentials in the intensity decay eq 2 with the time constants τ_A and τ_B, the equations for SAS of A and B becomes

$$\mathrm{SAS}_A(\lambda) = \frac{I_{SS}(\lambda)}{\tau_{ave}(\lambda)}\int_0^\infty a_\lambda[\mathrm{A}^*]_t\,\mathrm{d}t$$

$$\mathrm{SAS}_B(\lambda) = \frac{I_{SS}(\lambda)}{\tau_{ave}(\lambda)}\int_0^\infty b_\lambda[\mathrm{B}^*]_t\,\mathrm{d}t$$

where

$$\tau_{ave}(\lambda) = \int_0^\infty I_\lambda(t)\,\mathrm{d}t$$

i.e.,

$$\mathrm{SAS}_A(\lambda) = \frac{(\alpha_A(\lambda) + \alpha_B(\lambda))\tau_A I_{SS}(\lambda)}{\tau_{ave}(\lambda)}$$

$$\mathrm{SAS}_B(\lambda) = \frac{\alpha_B(\tau_B - \tau_A)I_{SS}(\lambda)}{\tau_{ave}(\lambda)} \quad (3)$$

These equations show that for determining species-associated spectra of A* and B*, there is no need to know the values of the individual rate constants k_A, k_B, and k_{AB} or the values of a_λ and b_λ.

The species-associated spectra of the two species were resolved from the steady-state spectra and the wavelength-dependent amplitudes of the two lifetimes using eq 3 in the case of Nile red in egg PC vesicles and SDS micelles. These are as shown in Figure 5. The species-associated spectra of A* and B* differ by about 10 nm in their emission maxima.

The analytical equations for the fluorescence intensity decay and the SAS were solved when there is a reversible reaction between A* and B*. The kinetic scheme for this is shown in Figure 4B. Let k_A and k_B represents the rate at which the two species A* and B* emit and k_{AB} and k_{BA} represent the forward and backward rates in the reaction equilibrium between A* and B*. In this case, the intensity decay equation becomes

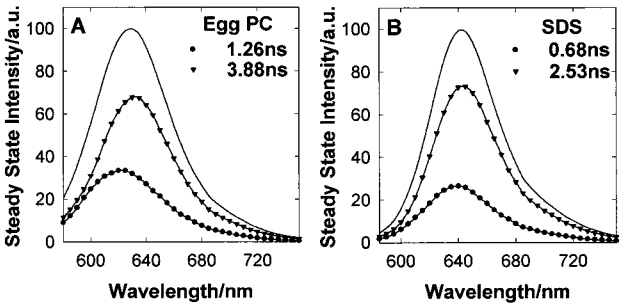

Figure 5. Species-associated spectra of Nile red in (A) egg PC vesicles and (B) SDS micelles in the case of irreversible reaction in the excited state (Figure 4A). Here, 1.26 and 3.88 ns represent the lifetimes of the initially excited species and the newly formed species in the case of Nile red in egg PC vesicles, whereas in the case of Nile red in SDS micelles, 0.68 and 2.53 ns correspond to the lifetimes of the initially excited and newly formed species, respectively.

$$I_\lambda(t) = [\mathrm{A}^*]_0\left[\exp\left[-\frac{(\mathrm{sk}+c)t}{2}\right]\times \left[\frac{a_\lambda(c+k_\mathrm{A}+k_\mathrm{AB}-k_\mathrm{B}-k_\mathrm{BA})}{2c}-\frac{b_\lambda k_\mathrm{AB}}{c}\right]+ \exp\left[-\frac{(\mathrm{sk}-c)t}{2}\right]\left[\frac{a_\lambda(c-k_\mathrm{A}-k_\mathrm{AB}+k_\mathrm{B}+k_\mathrm{BA})}{2c}+\frac{b_\lambda k_\mathrm{AB}}{c}\right]\right]$$

with

$$\mathrm{sk} = k_\mathrm{A}+k_\mathrm{B}+k_\mathrm{AB}+k_\mathrm{BA}$$

and

$$c = (k_\mathrm{A}^2+k_\mathrm{B}^2+k_\mathrm{AB}^2+k_\mathrm{BA}^2-2k_\mathrm{A}k_\mathrm{B}+2k_\mathrm{A}k_\mathrm{AB}- 2k_\mathrm{A}k_\mathrm{BA}-2k_\mathrm{B}k_\mathrm{AB}+2k_\mathrm{B}k_\mathrm{BA}+2k_\mathrm{AB}k_\mathrm{BA})^{1/2} \quad (4)$$

Here, the decay of the two species A* and B* is a double exponential at all emission wavelengths. The two decay constants in the intensity decay equation (eq 4) cannot be associated with any individual species, and all four rate constants affect the decay constants. If α_1 and α_2 represent the amplitudes and τ_1 and τ_2 represent the decay constants in the intensity decay eq 4, the species-associated spectra of the two species A* and B* become

$$\mathrm{SAS}_\mathrm{A}(\lambda) = (\alpha_1(\lambda)+\alpha_2(\lambda))(k_\mathrm{B}+k_\mathrm{BA})\tau_1\tau_2\frac{I_\mathrm{ss}(\lambda)}{\tau_\mathrm{ave}(\lambda)}$$

$$\mathrm{SAS}_\mathrm{B}(\lambda) = I_\mathrm{ss}(\lambda)-\mathrm{SAS}_\mathrm{A}(\lambda) \quad (5)$$

For resolving the species-associated spectra of the initially excited and newly formed species, one needs to know the value of $(k_\mathrm{B}+k_\mathrm{BA})$.

Lofroth[16] suggested a method to determine the value of $(k_\mathrm{B}+k_\mathrm{BA})$. From eq 5, one can write

$$k_\mathrm{B}+k_\mathrm{BA} = \frac{\mathrm{SAS}_\mathrm{A}(\lambda)\tau_\mathrm{ave}(\lambda)}{(\alpha_1(\lambda)+\delta\alpha_2(\lambda))\tau_1\tau_2 I_\mathrm{ss}(\lambda)}$$

and at the wavelengths where B* emission is negligible, $\mathrm{SAS}_\mathrm{A}(\lambda) \cong \mathrm{I}_\mathrm{SS}(\lambda)$ and hence,

$$k_\mathrm{B}+k_\mathrm{BA} \cong \frac{\tau_\mathrm{ave}(\lambda)}{(\alpha_1(\lambda)+\delta\alpha_2(\lambda))\tau_1\tau_2} \quad (6)$$

Hence, a quantity $(k_\mathrm{B}+k_\mathrm{BA})^\mathrm{app}$ is defined with the above

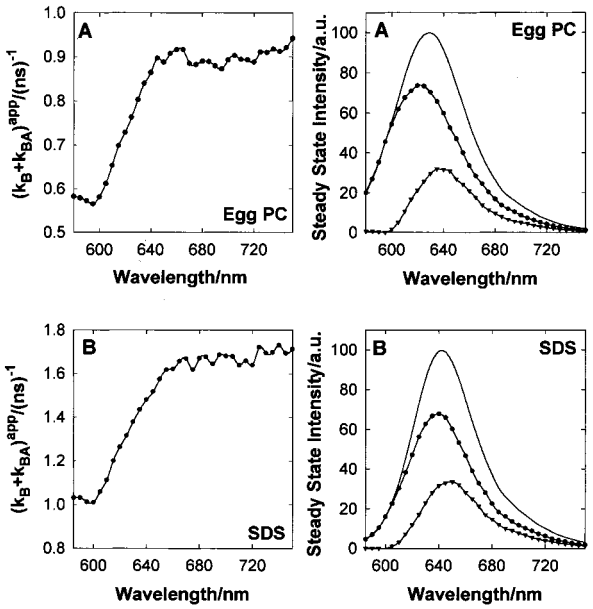

Figure 6. Plot of $(k_\mathrm{B}+k_\mathrm{BA})^\mathrm{app}$ with the emission wavelength and species-associated spectra (SAS) of the two species in the case of Nile red in (A) egg PC vesicles and (B) SDS micelles. The circles and triangles represent the SAS of the initially excited and newly formed species, respectively.

definition (eq 6), and from the plot of $(k_\mathrm{B}+k_\mathrm{BA})^\mathrm{app}$ versus the emission wavelength λ, the value of $(k_\mathrm{B}+k_\mathrm{BA})$ is obtained as the limiting value at the short end of the emission spectrum. A constant value for $(k_\mathrm{B}+k_\mathrm{BA})^\mathrm{app}$ in the blue end of the spectrum confirms the assumption that the emission from B* is negligible compared to that of A* in this region. $(k_\mathrm{B}+k_\mathrm{BA})$ cannot be determined in the cases where the spectra of A* and B* overlap at all emission wavelengths.

Figure 6 shows the plots of $(k_\mathrm{B}+k_\mathrm{BA})^\mathrm{app}$ as a function of the emission wavelength in the case of Nile red in egg PC vesicles and SDS micelles. The value of $(k_\mathrm{B}+k_\mathrm{BA})^\mathrm{app}$ approaches a constant value as we go toward lower emission wavelengths, and this value is taken as $(k_\mathrm{B}+k_\mathrm{BA})$ for determining SAS. The species-associated spectra for Nile red in egg PC vesicles and SDS micelles are as shown in Figure 6. The SAS of the two species differ by about 10 nm in their emission maxima as in the case of the irreversible reaction in the excited state (Figure 5).

Although the emission maxima of the two species A* and B* are almost the same whether the excited-state kinetics is reversible or irreversible, the relative spectral intensities of the two species get interchanged on the basis of the kinetics assumed (Figures 5 and 6). That means, in the case of an irreversible reaction between A* and B*, the spectral intensity of B* is higher than that of A*. In the other case, i.e., in the case of a reversible reaction between A* and B*, the spectral intensity of A* is higher than that of B*. The possible explanation for this change is that in the case of a reversible reaction, B* repopulates A* through a back reaction. It is not possible to identify whether the observed excited-state kinetics is irreversible or reversible solely on the basis of the fluorescence results.

Identity of the Newly Formed Species in the Excited State. One of the possible mechanisms in the excited state that can account for the excited-state kinetics of Nile red is the formation of a TICT state[6,8,11] where the charge transfer takes place from one end of the molecule to the other. The TICT state is formed from the initially excited planar state, and this process involves a bond-twisting mechanism in which the $-\mathrm{N(Et)_2}$ plane twists

perpendicular to the aromatic plane. The fluorescence spectra of the TICT state is generally red-shifted with respect to the normal planar state. The solvent plays a major role in the formation of the TICT state by stabilizing the initially excited nonpolar state and the polar TICT state to different extents. The TICT process is generally controlled by the solvent polarity rather than by the solvent viscosity.[17] In the case of Nile red, the rate of formation of TICT is reported to be very high in solvents whose solvent polarity parameter $E_T(30)$ exceeds a value of 46, i.e., in solvents that are polar compared to acetonitrile.[6] In the case of other solvents that are less polar, the TICT formation is expected to be low or absent. We have examined the fluorescence decays of Nile red in two solvents, *n*-hexane and chloroform, that are less polar compared to acetonitrile.

Nile red in *n*-hexane ($E_T(30) = 30.9$), which is a completely nonpolar solvent, exhibits a single fluorescence lifetime of 2.44 ns over the emission range 500−650 nm with the sample excited at 445 nm (emission maximum at 524 nm). In the case of chloroform ($E_T(30) = 39.1$), which is less polar compared to acetonitrile, Nile red (emission maximum at 598 nm) shows a single fluorescence lifetime of 4.33 ns over the emission range from 550 to 680 nm with the sample excited at 445 nm. In both the solvents, a short-lifetime component of about 0.2 ns was also observed at shorter emission wavelengths. More importantly, no negative amplitude for the short lifetime was observed at any emission wavelength, indicating the absence of excited-state kinetics in *n*-hexane and chloroform. The short lifetime observed in these two solvents is attributed to a ground-state heterogeneity of Nile red. This short lifetime is in qualitative agreement with the previous lifetime results reported for Nile red in *n*-heptane.[3] In the case of methanol ($E_T(30) = 55.5$), a single fluorescence lifetime (2.88 ns) was observed at all emission wavelengths. These results indicate that the TICT state of Nile red, if formed in any of the above solvents, is nonfluorescent. Hence, it is not the one responsible for the observed excited-state kinetics in membranes and micelles.

One other solvent that is less polar compared to acetonitrile and highly viscous is 1-octanol. The fluorescence intensity decay of Nile red in 1-octanol (emission maximum at 622 nm) is emission-wavelength-dependent. The multiple fluorescence intensity decays collected at various emission wavelengths ranging from 580 to 750 nm for an excitation wavelength of 570 nm can be globally fitted to a double-exponential function with the two lifetimes of 0.42 and 4.12 ns, and the amplitudes of the two lifetimes are wavelength-dependent. The amplitudes of the short lifetime (0.42 ns) become negative at emission wavelengths $\lambda_{em} \geq 625$ nm. The species-associated spectra for the two lifetimes in both cases of irreversible and reversible reaction in the excited state are as shown in Figure 7. The observation of negative amplitudes in a viscous organic solvent such as 1-octanol indicates that the observed excited-state kinetics of Nile red is viscosity-dependent.

The excited-state kinetics was also observed in the case of Nile red in another viscous solvent glycerol (emission maximum at 647 nm). The global analysis of multiple fluorescence decays collected at varying emission wavelengths ranging from 590 to 750 nm at an excitation wavelength of 570 nm gave two lifetimes of 0.56 and 2.63 ns with the amplitudes varying with the emission wavelength. Negative amplitudes were observed for the short-lifetime component (0.56 ns) at the emission wavelengths $\lambda_{em} \geq 650$ nm. The species-associated spectra for Nile red in glycerol are as shown in Figure 8.

The above experiments carried out on Nile red in different solvents suggest that the observation of dual lifetimes with negative amplitudes for the short lifetime at longer emission wavelengths is observed only in viscous solvents. Thus, the

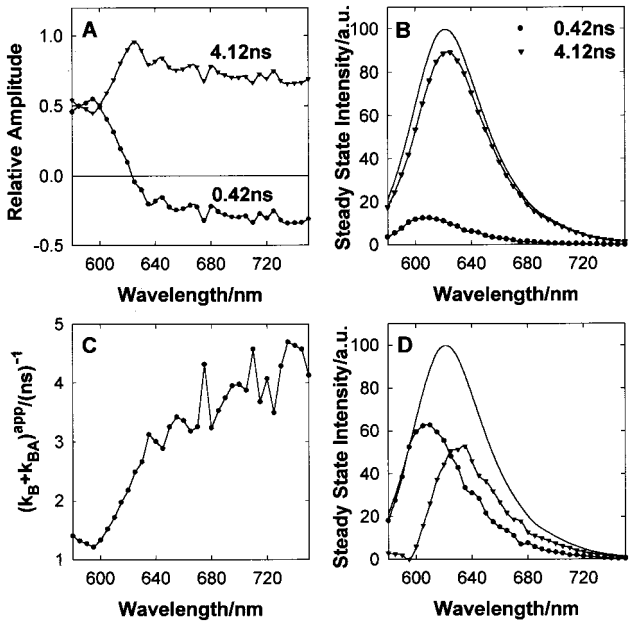

Figure 7. Nile red (0.77 μM) in 1-octanol: (A) relative amplitudes of the two lifetimes obtained by the global analysis of multiple fluorescence decays collected as a function of the emission wavelength at the excitation wavelength of 570 nm; (B) SAS in the case of irreversible reaction in the excited state, where 0.42 and 4.12 ns correspond to the lifetimes of the initially excited and newly formed species; (C) plot of $(k_B + k_{BA})^{app}$ with the emission wavelength; (D) SAS in the case of reversible reaction in the excited state. The circles and triangles represent the SAS of the initially excited and newly formed species, respectively.

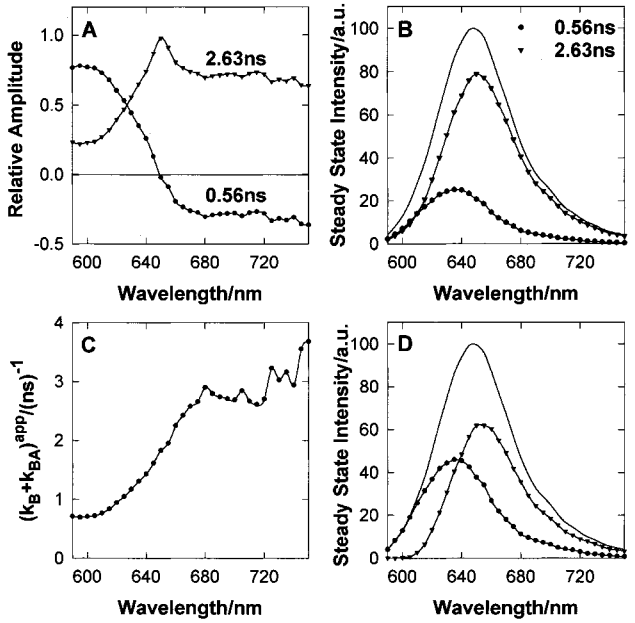

Figure 8. Nile red (0.77μM) in glycerol: (A) relative amplitudes of the two lifetimes obtained by the global analysis of multiple fluorescence decays collected as a function of the emission wavelength at the excitation wavelength of 570 nm; (B) SAS in the case of irreversible reaction in the excited state, where 0.56 and 2.63 ns correspond to the lifetimes of the initially excited and newly formed species; (C) plot of $(k_B + k_{BA})^{app}$ with the emission wavelength; (D) SAS in the case of reversible reaction in the excited state. The circles and triangles represent the SAS of the initially excited and newly formed species, respectively.

excited-state kinetics of Nile red is solvent-viscosity-dependent and not polarity-dependent.

The viscosity-dependent excited-state kinetics is more likely to be the solvent relaxation where the initially excited state relaxes to a solvent relaxed state.[18] For a molecule whose dipole moments in the ground state and excited state are considerably different, there occurs a sudden change in electronic charge distribution upon excitation. The solvent responds to this change by a reorganization of the solvent dipoles around the fluorophore. The time scale of this solvent relaxation depends on the properties of the solvent.[18] In the case of Nile red, the change in the dipole moment upon excitation was estimated to be 11.6 D from the solvatochromic Stoke's shift with the solvent polarity using the Lippert−Mataga equation.[10] This large change in the dipole moment results in reorganization of the solvent dipoles around Nile red in the excited state. This relaxation process is generally of the order of a few tens of picoseconds in pure solvents of low viscosity and increases with an increase of viscosity of the medium.[18] When the solvent relaxation is comparable to or slower in time than the fluorescence decay of the initially excited state, one can observe emission from the initially excited state and the solvent relaxed states.

Excited-state solvent relaxation can be either a continuous solvent relaxation or a two-state relaxation.[18] If the solvent relaxation is continuous, the fluorescence lifetimes should be emission-wavelength-dependent. If we observe two lifetimes that are constant over the emission spectrum with only the relative amplitudes varying with the emission wavelength, then the solvent relaxation is of the two-state model. The observation of two lifetimes that are constant over all emission wavelengths and of negative amplitudes in viscous organic solvents such as 1-octanol and glycerol supports the two-state solvent relaxation in the excited state as a possible mechanism for the observed excited-state kinetics. Hence, the short and long lifetimes observed in the case of Nile red in egg PC vesicles and SDS micelles correspond to the initially excited and solvent relaxed species, respectively.

Time-Resolved Emission Spectra. Excited-state solvent relaxation can also be studied by using the method of time-resolved emission spectra (TRES).[19,20−22] The TRES is constructed from the fluorescence decays collected at different wavelengths using the procedure described in ref 19. The emission intensity at the wavelength λ at time $t = t'$ was given by

$$I_\lambda(t') = \frac{I_{ss}^\lambda}{\tau_{ave}^\lambda}\sum_{i=1}^{2}\alpha_i^\lambda \exp(-t'/\tau_i) \qquad (7)$$

where α_i^λ are the wavelength-dependent amplitudes of the two lifetimes τ_i. τ_{ave}^λ is the average lifetime ($=\sum_i \alpha_i^\lambda \tau_i$), and I_{SS}^λ is the steady-state intensity at wavelength λ. The time-resolved spectral data were fitted to a log-normal line-shape function[19] defined by eq 8 to obtain a smooth spectrum.

$$g(\upsilon) = g_0 \exp\left\{-\ln(2)\left(\frac{\ln[1+\alpha]}{b}\right)^2\right\} \qquad \text{for } \alpha > 1$$
$$= 0 \qquad \text{for } \alpha \le 1 \qquad (8)$$

where $\alpha = 2b(\nu - \nu_{max})/\Delta$ and g_0, ν_{max}, and b represent the peak height, peak frequency, and asymmetry factor, respectively. Figure 9 shows the variation in the fluorescence emission maximum ν_{max} with time after excitation for the four systems: Nile red in octanol, glycerol, SDS micelles, and egg PC membranes. The variation follows a single-exponential behavior, and the estimated solvation times were 0.51, 0.72, 0.84, and 1.72 ns for Nile red in octanol, glycerol, SDS micelles, and egg PC membranes, respectively. In the case of systems that follow a continuous solvent relaxation mechanism, the time-dependent emission maximum does not follow single-exponential behavior and it generally shows multiple solvation times.[19,20,22] Moreover, if the solvent relaxation is of continuous type, then the width of the TRES constructed at different times after excitation should be the same. This is not observed in the case of Nile red in the above four systems. All these strongly agree with the conclusion drawn earlier from SAS measurements that the excited-state kinetics of Nile red follows a two-state model. An energy level diagram appropriate for the excited-state kinetics of Nile red in viscous solvents, micelles, and membranes is shown in Figure 10.

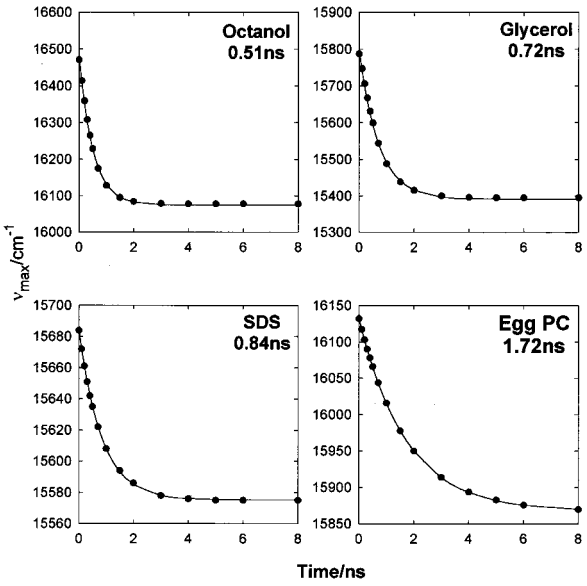

Figure 9. Variation of the fluorescence emission maximum of Nile red in octanol, glycerol, SDS micelles, and egg PC membranes with time. The variation follows single-exponential behavior, and the respective solvation times are indicated on the plots.

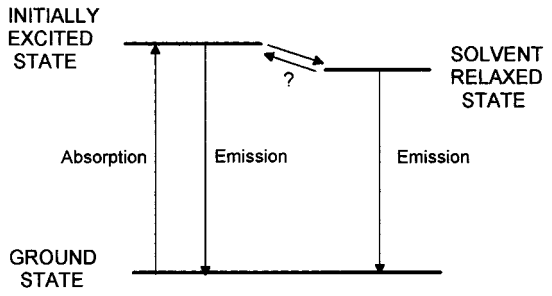

Figure 10. Proposed energy level diagram of Nile red to explain the dual emission of Nile red in membranes, micelles, and viscous organic solvents.

The excited-state kinetics of Nile red is similar to that observed in the case of aminocoumarins in alcohol solvents.[23] In this case, similar to the case of Nile red, the decay-associated spectra (DAS) analysis clearly shows that the excited-state solvent relaxation follows a two-state model and that the time-dependent emission maximum exhibits a single-exponential behavior. For distinguishing between a two-state or continuous solvent relaxation model, the method of DAS or SAS is best suited compared to the method of TRES. In the two-state model, the solvent relaxation can be represented as DAS/SAS of the

two lifetimes, those of the initially excited state and the solvent relaxed state, which are kinetically coupled.

The dynamic solvent effects during the lifetime of the excited dipole where the solvent exerts a time-dependent dielectric friction is known to affect the isomerization reactions, electron- and proton-transfer reactions, and other charge-transfer reactions.[20,24,25] Much more needs to be understood regarding these dynamic solvent effects on the theoretical side.[26,25] In this article, we report the excited-state kinetics of Nile red in membranes, micelles, and viscous organic solvents that follow a two-state model with the help of SAS measurements.

Summary

The fluorescence decays collected at different emission wavelengths in the case of Nile red in egg PC vesicles and SDS micelles are emission-wavelength-dependent. The global analysis of these decays resulted in two lifetimes with negative amplitudes for the short-lifetime component at long emission wavelengths. Observation of negative amplitudes is the characteristic signature for excited-state kinetics. This excited-state kinetics is also observed in the case of viscous organic solvents such as 1-octanol and glycerol and is attributed to that of an excited-state solvent relaxation. An energy level diagram was proposed for the excited-state kinetics of Nile red.

Acknowledgment. The author thanks Prof. N. Periasamy for many helpful discussions, advice, and critical reading of the manuscript.

References and Notes

(1) (a) Romoino, P.; Margallo, E.; Nicolo, G. *J. Lipid Res.* **1996**, *37*, 1207. (b) Kinnunen, P. K.; Rytono, M.; Koiv, A.; Lehtonan, J.; Mustonan, P.; Aro, A. *Chem. Phys. Lipids* **1993**, *66*, 75.

(2) (a) Maiti, N. C.; Krishna, M. M. G.; Britto, P. J.; Periasamy, N. *J. Phys. Chem. B* **1997**, *101*, 11051. (b) Sarkar, N.; Datta, A.; Das, S.; Bhattacharya, K. *J. Phys. Chem.* **1996**, *100*, 15483.

(3) Datta, A.; Mandal, D.; Pal, S. K.; Bhattacharya, K. *J. Phys. Chem. B* **1997**, *101*, 10221.

(4) (a) Ruvinov, S. B.; Yang, X. J.; Parris, K. D.; Banik, U.; Ahmed, S. A.; Miles, E. W.; Sackett, D. L. *J. Biol. Chem.* **1995**, *270*, 6357. (b) Sackett, D. L.; Knutson, J. R.; Wolff, J. *J. Biol. Chem.* **1990,** *265*, 14899.

(5) Greenspan, P.; Mayer, E. P.; Fowler, S. D. *J. Cell Biol.* **1985**, *100*, 965.

(6) Sarkar, N.; Das, K.; Nath, D. N.; Bhattacharya, K. *Langmuir* **1994**, *10*, 326.

(7) Choi, M.; Jin, D.; Kim, H.; Kang, T. J.; Jeoung, S. C.; Kim, D. *J. Phys. Chem. B* **1997**, *101*, 8092.

(8) Dutta, A. K.; Kamada, K.; Ohta, K. *Chem. Phys. Lett.* **1996**, *258*, 369.

(9) Ira; Krishnamoorthy, G. *Biochim. Biophys. Acta* **1998**, *1414*, 255.

(10) (a) Dutt, G. B.; Doraiswamy, S.; Periasamy, N.; Venkataraman, B. *J. Chem. Phys.* **1990**, *93*, 8498. (b) Dutt, G. B.; Doraiswamy, S.; Periasamy, N. *J. Chem. Phys.* **1991**, *94*, 5360.

(11) Dutta, A. K.; Kamada, K.; Ohta, K. *J. Photochem. Photobiol. A* **1996**, *93*, 57.

(12) Sackett, D. L.; Wolff, J. *Anal. Biochem.* **1987**, *167*, 228.

(13) Krishna, M. M. G.; Periasamy, N. *J. Fluoresc.* **1998**, *8*, 81.

(14) Periasamy, N.; Doraiswamy, S.; Maiya, B. G.; Venkataraman, B. *J. Chem. Phys.* **1988**, *88*, 1638.

(15) Knutson, J. R.; Beechem, J. M.; Brand, L. *Chem. Phys. Lett.* **1983**, *102*, 501.

(16) Lofroth, J. *J. Phys. Chem.* **1986**, *90*, 1160.

(17) Hicks, J.; Vandersall, M.; Babarogic, Z.; Eisenthal, K. B. *Chem. Phys. Lett.* **1985**, *116*, 18.

(18) Lakowicz, J. R. *Principles of Fluorescence Spectroscopy*; Plenum: New York, 1983.

(19) Maroncelli, M.; Fleming, G. R. *J. Chem. Phys.* **1987**, *86*, 6221.

(20) Maroncelli, M.; MacInnis, J.; Fleming, G. R. *Science* **1989**, *243*, 1674.

(21) Vajda, S.; Jimenez, R.; Rosenthal, S. J.; Fidler, V.; Fleming, G. R.; Castner, E. W., Jr. *J. Chem. Soc., Faraday Trans.* **1995**, *91*, 867.

(22) Rocker, C.; Heilemann, A.; Fromherz, P. *J. Phys. Chem.* **1996**, *100*, 12172.

(23) Yip, R. W.; Wen, Y. X.; Szabo, A. G. *J. Phys. Chem.* **1993**, *97*, 10458.

(24) (a) Barbara, P. F.; Jarzeba, W. *Acc. Chem. Res.* **1988**, *21*, 195. (b) Barbara, P. F.; Walker, G. C.; Smith, T. P. *Science* **1992**, *256*, 975. (c) Reid, P. J.; Barbara, P. F. *J. Phys. Chem.* **1995**, *99*, 3554.

(25) Bagchi, B. *Curr. Sci.* **1995**, *69*, 129.

(26) (a) Bagchi, B. *Annu. Rev. Phys. Chem.* **1989**, *40*, 115. (b) Bagchi, B.; Chandra, A. *Int. J. Mod. Phys. B* **1991**, *5*, 461.